*Supporting Information for*

# Aptamer-conjugated $Mn_3O_4$@$SiO_2$ Core-Shell Nanoprobes for Targeted Magnetic Resonance Imaging

He Hu[a], Antao Dai[a], Jin Sun[a], Xiangyuan Li[a], Fenghou Gao[b], Lizhong Wu[b], Yong Fang[b]*, Hong Yang[a], Lu An[a], Huixia Wu[a], Shiping Yang[a]*

[a]The Education Ministry Key Lab of Resource Chemistry and Shanghai Key Laboratory of Rare Earth Functional Materials, Department of Chemistry, Shanghai Normal University, No.100 Guilin Road, Shanghai, 200234, China

[b]No. 3, People's Hospital Affiliated to Shanghai Jiao Tong University School of Medicine, Shanghai 201900, China

E-mail: fangyong1020@hotmail.com, shipingy@shnu.edu.cn

| | | Size (d.nm): | % Number | Width (d.nm): |
|---|---|---|---|---|
| Z-Average (d.nm): 39.2 | Peak 1: | 37.51 | 100.0 | 6.563 |
| PdI: 0.619 | Peak 2: | 0.000 | 0.0 | 0.000 |
| Intercept: 0.244 | Peak 3: | 0.000 | 0.0 | 0.000 |

Result quality : Good

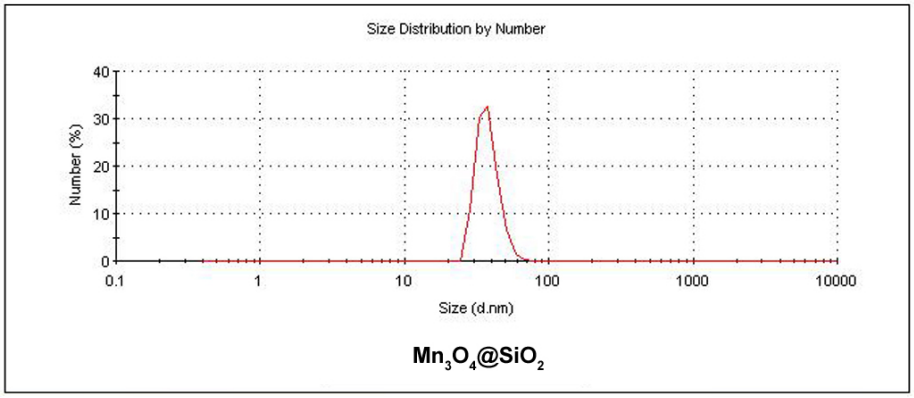


| | | Size (d.nm): | % Number | Width (d.nm): |
|---|---|---|---|---|
| Z-Average (d.nm): 53.15 | Peak 1: | 50.16 | 100.0 | 12.77 |
| PdI: 0.113 | Peak 2: | 0.000 | 0.0 | 0.000 |
| Intercept: 0.786 | Peak 3: | 0.000 | 0.0 | 0.000 |

Result quality : Good

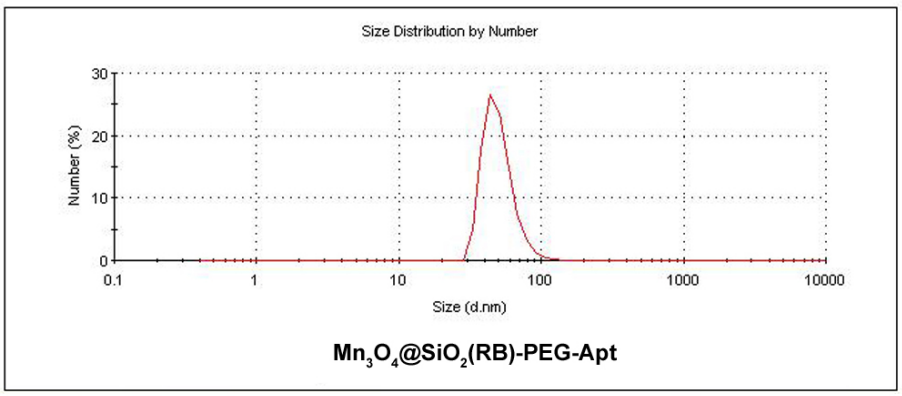


Figure S1. The effective hydrodynamic diameter of the core-shell $Mn_3O_4$@$SiO_2$ and $Mn_3O_4$@$SiO_2$(RB)-PEG-Apt measured by dynamic light scattering (DLS).

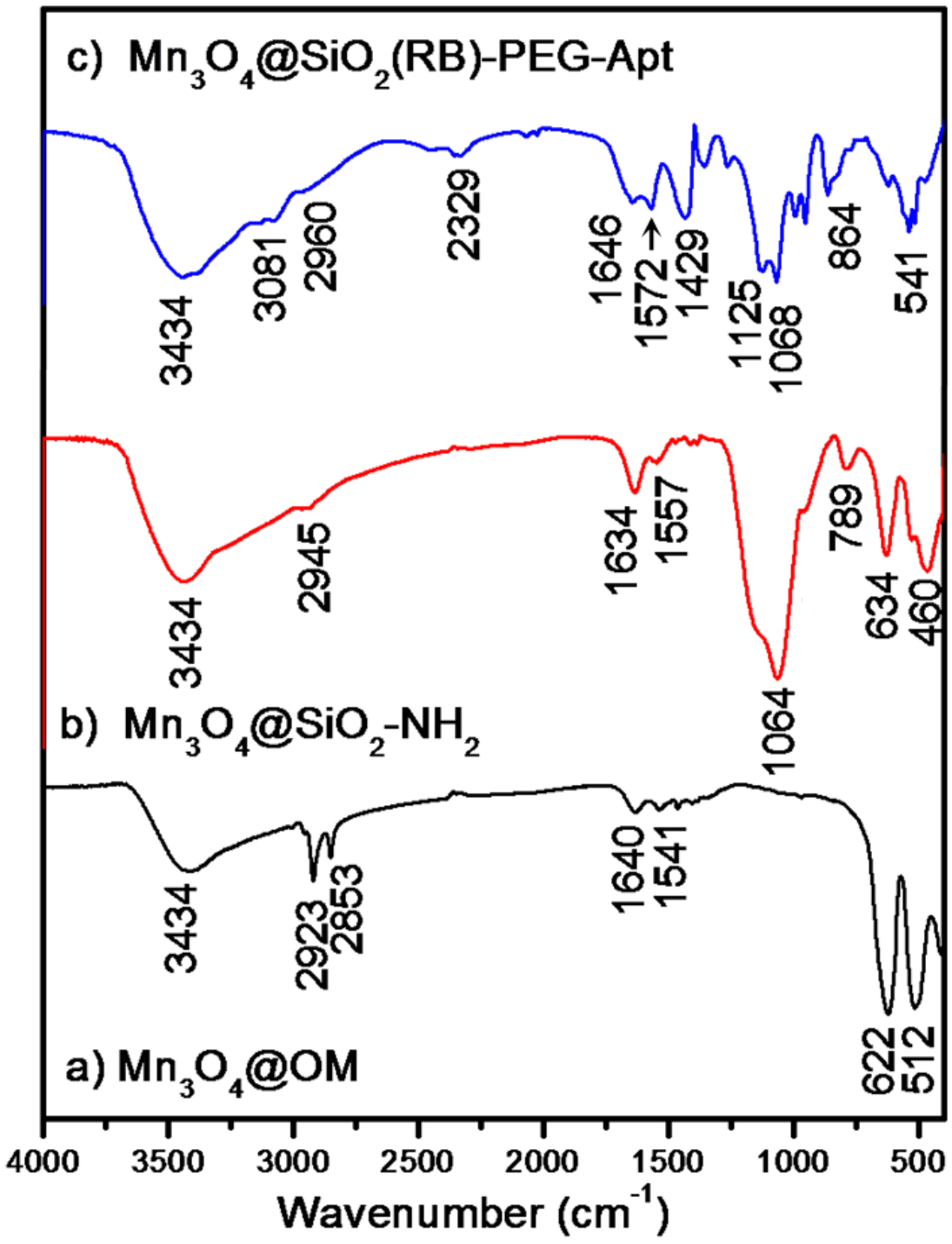


**Figure S2**. FTIR spectra of A) $Mn_3O_4$ NPs, B) $Mn_3O_4$@$SiO_2$-$NH_2$ core-shell nanocomposites and c) $Mn_3O_4$@$SiO_2$(RB)-PEG-Apt.

The broad band at around $\nu$ = 3434 $cm^{-1}$ corresponds to the –N-H and O–H stretching vibration are observed from the as-prepared sample. As shown in Figue S2a, the peaks at 2923 and 2853 $cm^{-1}$ are assigned to the asymmetric ($v_{as}$) and symmetric ($v_s$) stretching vibrations of methylene (–$CH_2$) in the long alkyl chain of OM. The peaks at 1640, 1541, 622, and 512 $cm^{-1}$ should be attributed to the Mn-N or Mn-O absorption band. After silica coating (Figure S2b), the strong and broad band in the range of 1230 ~1010 $cm^{-1}$and a relative weak peak at 460 $cm^{-1}$, corresponding to the Si-O-Si asymmetric ($v_{as}$) stretching vibration from the $SiO_2$ matrix. The transmission bands at $\nu$ = 2945, 789, and 634 $cm^{-1}$ assign to the asymmetric ($v_{as}$) and symmetric ($v_s$) stretching vibrations of methylene ($CH_2$) from the hydrolysis and condensation of -Si-$(CH_2)_2$-$NH_2$ of APTES, respectively. The characteristic absorption peak at 1634 $cm^{-1}$ can be assigned to N-H deformation vibrations. After the core-shell nanoparticle further conjugated with RBITC, PEG and Aptamer (Figure S2c), the large amount of organnic ligands on the surface of the NPs resulting the stretching vibrations of methylene ($CH_2$) (around $\nu$ = 3081, 2960, and 864 $cm^{-1}$) increased dramaticaly. the new peaks at $\nu$ =2329, 1646, 1572 and 1640 $cm^{-1}$ attributed to the vibration of imide-bond appear in aptamer molecular and formation between the amines and carboxylic acid of PEG. the strong and broad band in the range of 1230 ~1010 $cm^{-1}$ is slightly different from the silcia coated $Mn_3O_4$ NPs is due to the overlap of the C-O-C stretching vibration from the PEG and Si-O-Si asymmetric ($v_{as}$) stretching vibration from the $SiO_2$ matrix.

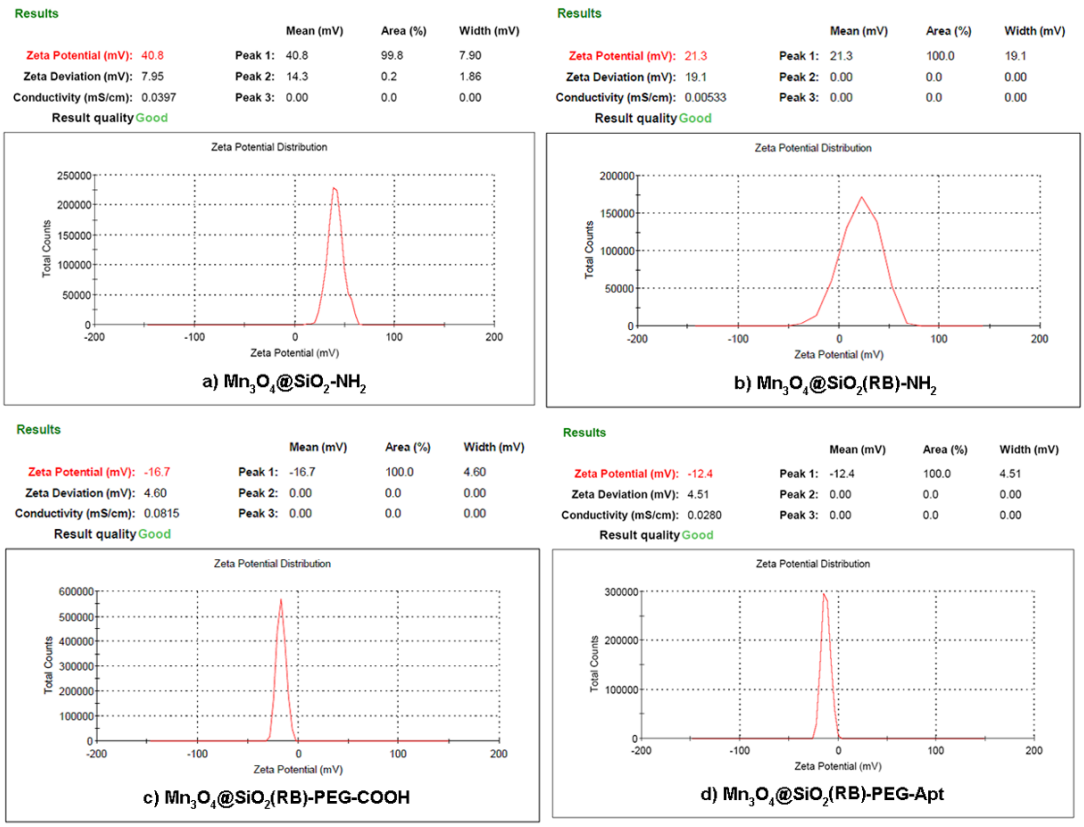


**Figure S3**. The surface zeta potential of a) $Mn_3O_4$@$SiO_2$-$NH_2$, b) $Mn_3O_4$@$SiO_2$(RB)-$NH_2$, c) $Mn_3O_4$@$SiO_2$(RB)-PEG-COOH, d) $Mn_3O_4$@$SiO_2$(RB)-PEG-Apt.

As well known, the surface zeta potential of pure $SiO_2$ hollow spheres was about – 49 mV, while the amine-functionalized $Mn_3O_4$@$SiO_2$ core-shell nanocomposites were increased to +40.8 mV, and the value was reduced to +20.3 mV after one-third of amines conjugated with RBITC, and the value was reduced to -16.7 mV after PEG-COOH conjugated with the remaining amines. After formation of the final $Mn_3O_4$@$SiO_2$(RB)-PEG-Apt products, the zeta potential was -12.4 mV.

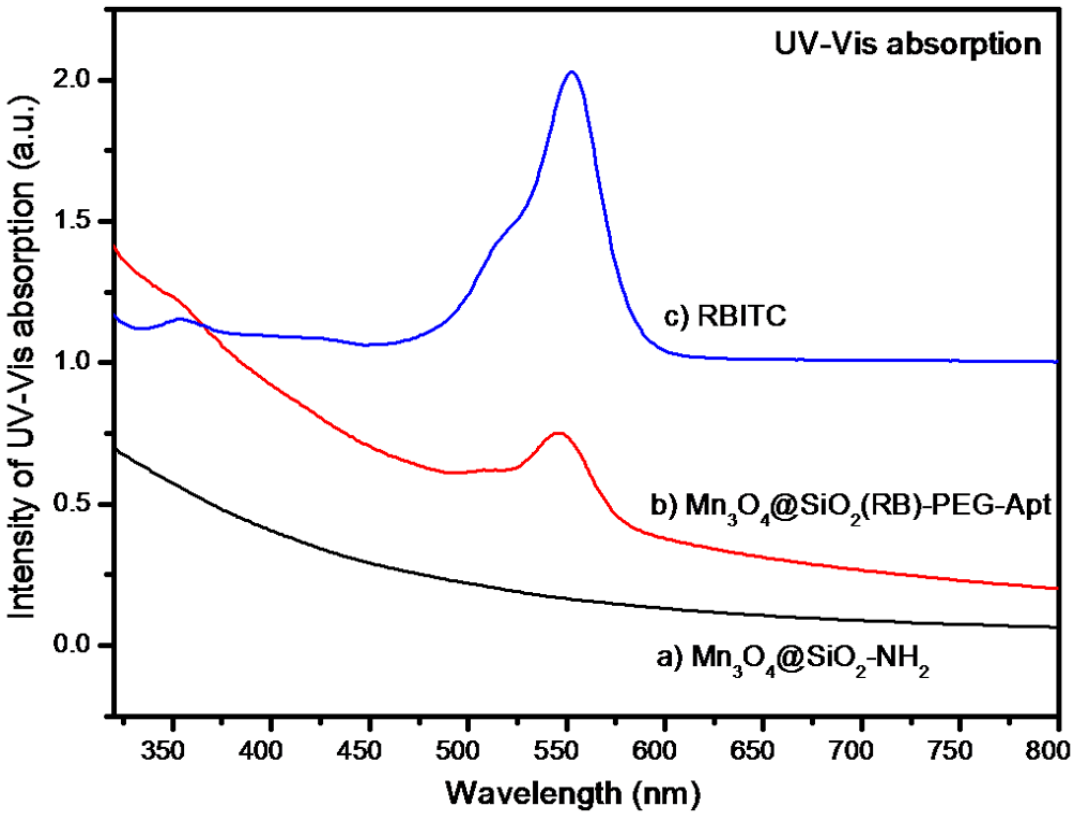


**Figure S4**. UV–vis spectra of A) $Mn_3O_4$@$SiO_2$-$NH_2$ nanocomposites, B) $Mn_3O_4$@$SiO_2$(RB)-PEG-Apt and C) pure RBITC in PBS buffer. It is clear that $Mn_3O_4$@$SiO_2$-$NH_2$ nanocomposites do not show any prominent absorption peaks, and the characteristic bands at 550 nm correspond to the absorption of the dye Rhodamine B.

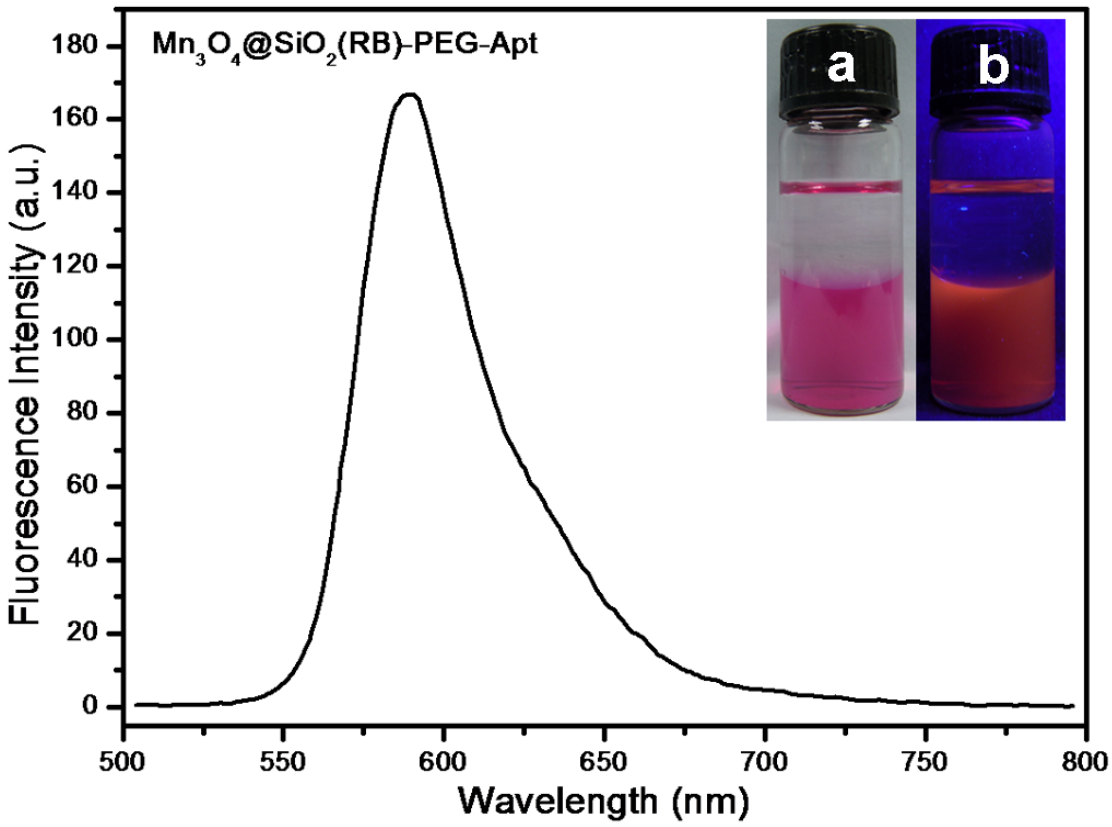


**Figure S5**. The room temperature photoluminescence (PL) spectra of $Mn_3O_4$@$SiO_2$(RB)-PEG-Apt with concentration of 100 μg $mL^{-1}$ in aqueous excited at 488 nm. Insets: visual photographs of $Mn_3O_4$@$SiO_2$(RB)-PEG-Apt nanocomposites in a) PBS at the bottom (hexane at the upper layer), and the b) red emission of Rhodamine B under the 365nm portable UV lamp excitation.

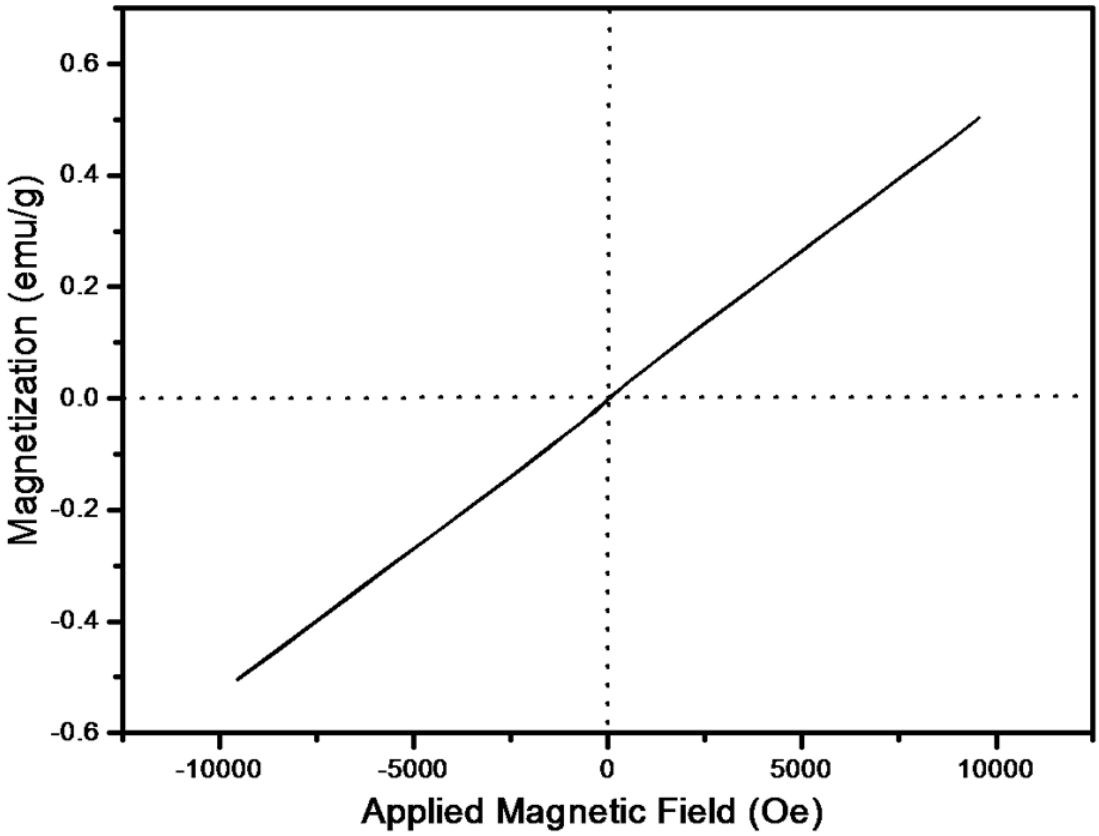


**Figure S6**. Hysteresis loops of $Mn_3O_4$@$SiO_2$(RB)-$NH_2$ NPs at T = 300 k. They were paramagnetic at room temperature.

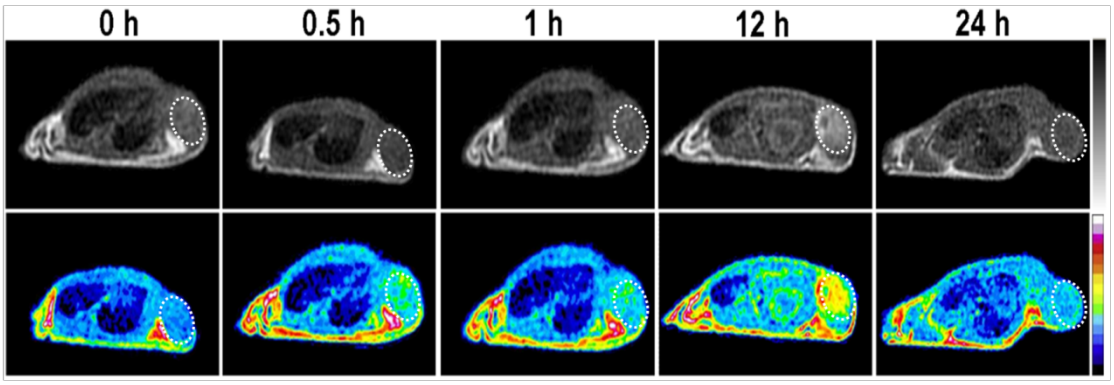


**Figure S7**. The target group of $T_1$-weight MR images of a tumor bearing mouse model (inoculated with HeLa cells) injected with $Mn_3O_4$@$SiO_2$(RB)-PEG-Apt NPs, obtained at pre, 0.5, 1, 12, and 24 h post-injection. The upper panel shows the black and white images, the bottom panel shows the colored images (the color bar changing from black to white indicates the gradual increase in MR signal intensity).

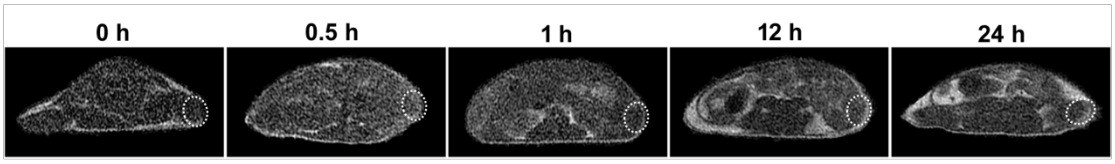


**Figure S8**. The control group of $T_1$-weight MR images of a tumor bearing mouse model (inoculated with HeLa cells) injected with $Mn_3O_4$@$SiO_2$(RB)-PEG NPs, obtained at pre, 0.5, 1, 12, and 24 h post-injection. There were nearly no contrast enhancement in tumor throughout the observation time.